



## Development of in-situ fatigue crack observing system for rotating bending fatigue testing machine

B. Lian

*Yamamoto Metal Technos Co., Ltd.*

A. Ueno

*Ritsumeikan University, 1-1-1 Noji-higashi, Kusatsu, Shiga 525-8577, Japan*

*ueno01@fc.ritsumei.ac.jp*

T. Iwashita

*Graduate School Student of Ritsumeikan University*

---

**ABSTRACT.** To substitute for a traditional replication technique, an *in-situ* fatigue crack observing system for rotating bending testing machine has been newly developed. For verifying performance of this observing system, fatigue tests were carried out by using fatigue specimen having a small artificial defect. It is proved that this system can be detect a small fatigue crack and its propagation behavior.

**KEYWORDS.** In-situ observation; Fatigue crack initiation; Fatigue crack propagation; Rotating bending testing machine.

---

### INTRODUCTION

In the field of the fatigue properties of metallic materials, the assessment of the  $S-N$  curve, which consists to the stress level and the number of cycles up to failure, does not give an entire viewpoint of the phenomenon. Indeed, a lot of information on the fatigue properties can be gathered by the observation of the fatigue crack initiation and propagation directly on the specimen surface. Unlike the case of pre-cracked specimens used for fracture mechanics experiments, the initiation and the propagation of the conventional fatigue specimens are often investigated by replica methods. Due to the performances of replica made of cellulose acetate film good enough to duplicate the specimen surface, it is possible to detect very small fatigue crack just after the initiation. However, it is necessary to have some experience on the use of this technique, in addition there are also cases where the utilization of replica is complex. It is particularly the case for fatigue specimens designed for rotating bending tests, with an hourglass shape at the minimum cross section spot.

Nevertheless, performances of some optic devices have been improved in the latest years, in the field of: (i) affordable long working distance microscopy, (ii) high-definition video camera, and (iii) high brightness LED components. The combination of these new developments gives the possibility to design a system adapted for fatigue rotating bending tests, and thus to observe continuously the fatigue crack propagation.

---

This paper deals first with an explanation of the optical system designed here, then some fatigue crack observation results obtained are also introduced.

## SYSTEM OUTLINE

### *Optic-System*

In the case of the rotating bending fatigue tests, since the fatigue specimen at the minimum cross section is incurvated, if the axis of microscope is the same as the axis enlightenment of the specimen, only the summit of the specimen will be observable, as shown in Fig. 1(a). Such a configuration is not suitable to obtain the full image of the entire crack on the specimen surface. Nevertheless, by adopting a configuration where several light sources are circularly placed around the fatigue specimen, it is possible to enlighten favorably a larger zone, as in Fig. 1(b).

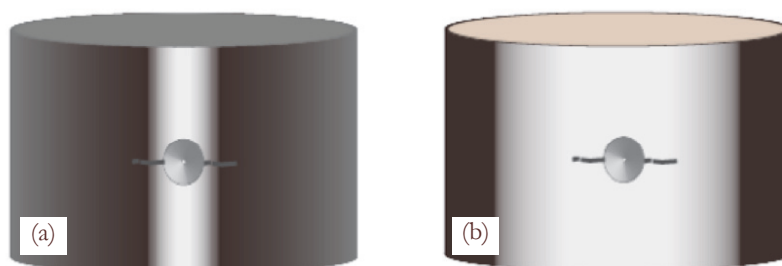


Figure 1: Schematics of lighting. (a): In case of point light source, (b): In case of surround light source.

In order to get observation in adequate synchronization with the rotation speed of the fatigue test, stroboscope device is usually set in order to make the observation of the highest position of the fatigue specimen, where the maximum tension stress level is reached. However, in the case of conventional stroboscope with xenon lamp components, the directive signal of flash, in other words the pulse frequency, is initially set, since the lamps' flash and the pulse frequency is not totally in agreement. Thus, the timing of the observation will be shifted, resulting in a loss of luminosity compared to the optimum position for crack observation. To solve this problem, use of stroboscope with high luminosity LED components gives a more favorable observation condition than conventional stroboscope. In the rest of this paper, the introduced system gave acceptable observation conditions by setting the flash directive signal. Indeed, even though the flash period was extremely short, the luminosity given out by white color high luminosity LED, arranged on circuit boards illustrated in Fig. 2(a), was sufficient. More precisely, two circuit boards were installed around the specimen, as indicated in Fig. 2(b).

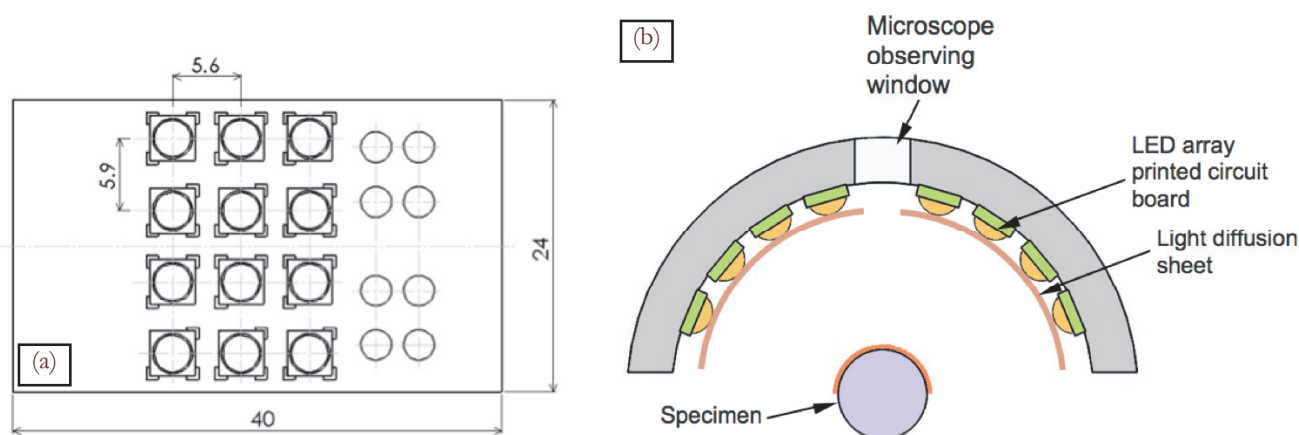


Figure 2: LED type stroboscope. (a): LED array plan, (b): Arrangement plan.

### Control and Configuration Equipment of the Introduced System

Outline of the system dedicated to the control of the LED stroboscope's flash timing is schematically depicted in Fig. 3. This system is composed of (1) the motor and the spindle that is controlling the rotation of the fatigue specimen, (2) the timing gear at opposite side of the specimen is also rotated in the same way, (3) the magnetic sensor placed in the vicinity of the gear, (4) the servo-motor, which is introduced here to set the position of the magnetic sensor at any angular position around the gear, (5) the control system that gives the flash directive signal (pulse frequency) to the LED stroboscope, (6) the high-definition digital video camera, which records at a predetermined interval of time, (7) the long working distance microscope, and (8) the personal computer to record and analyze the data obtained.

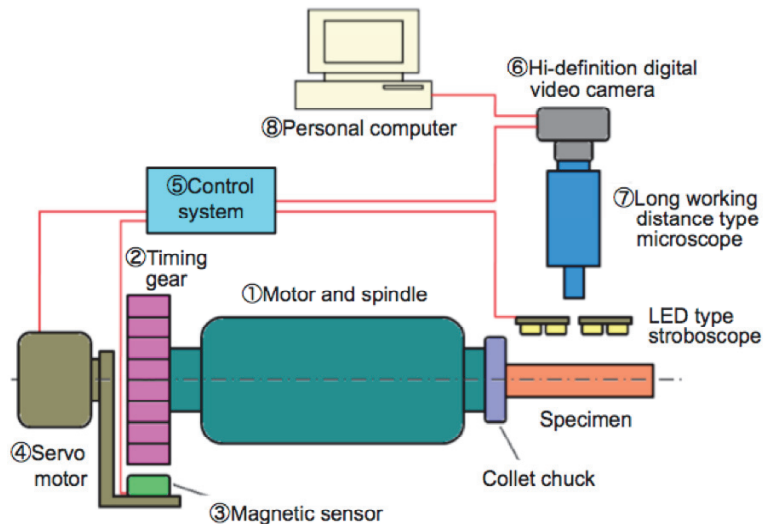


Figure 3: Schematic of system components.

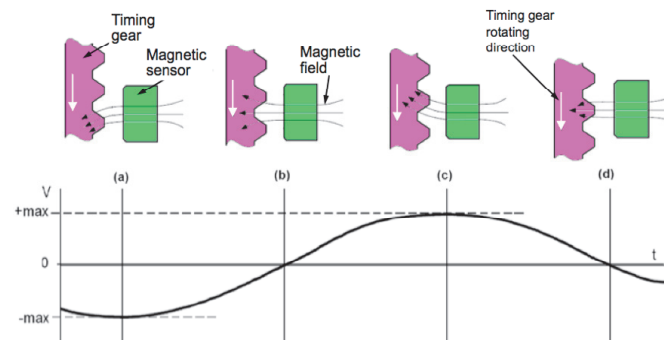


Figure 4: Relationship between magnetic sensor position and output voltage signal.

Depending on the relative position of the timing gear's tooth, the magnetic field of the magnetic sensor will change. Thus, it is possible to determine the position of the gear according to the output voltage signal from the sensor, as one can see in Fig. 4. Indeed, the magneto resistance elements inside the sensor will induce a different resistance value depending on the magnetic field. Since the resistance value change conducts to a variation of the voltage, the output voltage from the magnetic sensor will show a sinusoidal shape function against time. After treatment by the control system, one can obtain the pulse signal (or the digital signal), which is given to the LED stroboscope to flash at the appropriate timing. In addition, it is possible to adjust the flash period by changing the threshold value when converting the pulse signal. Therefore, one can adjust with an error as slight as possible the microscope observation field flashed by LED stroboscope, in accordance with the rotation speed of the rotating bending fatigue machine.

Timing of the LED flashing is determined by the position of the tooth of the gear and the magnetic sensor around the gear at an angle controlled by a servo motor, as shown in Fig. 5. The LED stroboscope flashes in a short time lapse at the time of the sensor detects that the tooth A is approaching. In the Fig. 5(a), since the sensor angular position is 1, when the

tooth A is detected, the LED stroboscope flashes for a lapse time the position indicated by plain star. If the position of the magnetic sensor is changed to position 2, the LED stroboscope will flash for a lapse time the position indicated by hollow star. Thus, it is possible to adjust the flash timing over these 4 possible angular positions of the magnetic detector. As depicted in Fig. 5, as the gear used here consists of 9 teeth, in the case where there are 4 possible angular positions of the magnetic sensor, we can flash at 36 different angular positions, which means an angular interval between two positions of  $10^\circ$ . One can note that we can reduce such an angular interval by introducing more possible angular positions of the magnetic sensor, or installing a gear with a higher number of teeth.

In the case where an artificial defect has been added at the surface of the fatigue specimen, since the crack initiation site is already known, we are in the case depicted in the Fig. 5(a), where the same angular position of the magnetic sensor will be used for the duration of the fatigue test. Nevertheless, if the crack initiation site is unknown, after initiation of the crack, it is possible to switch over the possible angular positions of the magnetic sensor in order to have an appropriate flash timing. However, between fatigue test's start and detection of the crack initiation, the interval meter of the video camera have to record the time interval in order to obtain the number of fatigue cycle data, which is mandatory to get appropriate results.

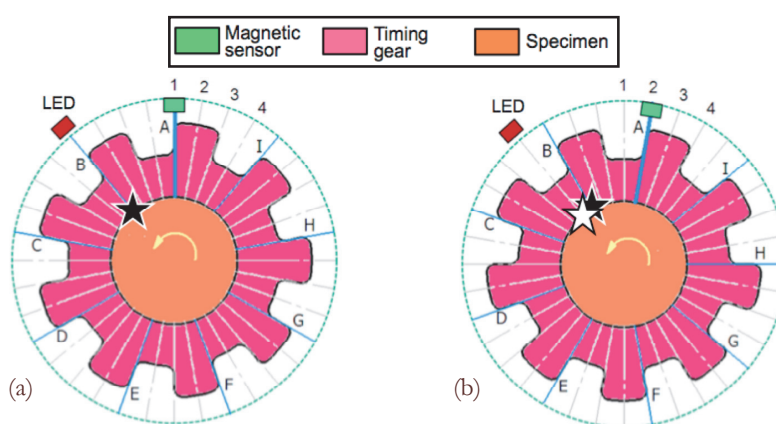


Figure 5: How to set up LED flushing timing. (a): Case 1 for fixed point observation, (b): Case 2 for circumference observation.

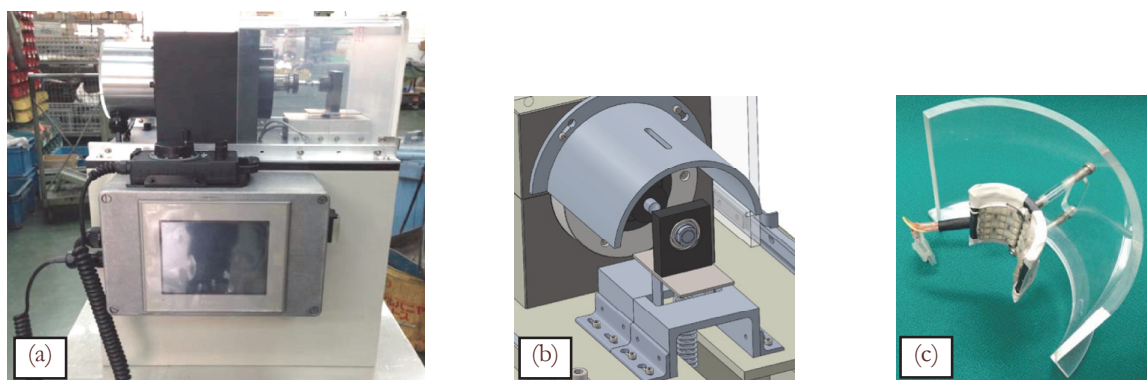


Figure 6: Newly developed high-speed rotating bending fatigue testing machine. (a): Side view photograph, (b): 3D-CAD image near specimen end, (c): LED type stroboscope and attachment cover.

### Rotating Bending Testing Machine

The fatigue crack observation system previously introduced can be adapted to all types of rotating bending testing machine. In this study, the system was installed on a single axis spin motor high speed rotating bending machine as one can see in Fig. 6. The overview of the testing machine, details on the environment close to the hanging weight and a photo of the LED stroboscope and its plastic cover are given in Fig 6(a), (b) and (c), respectively. For this machine, motor engine is designed for machine tool usage. Thus, it is possible to reach loading frequency up to 500 Hz ( $\approx 30,000$  rpm), however since the chuck of the fatigue specimen is directly integrated in the principal axis of the motor, the fatigue specimen must have a very low eccentricity characteristic.

### EVALUATION OF THE PERFORMANCE OF THE INTRODUCED SYSTEM

In order to assess the performances of this system, fatigue tests were carried out on valve spring Si-Cr oil tempered wire SWOSC-V[2]. Configuration of the fatigue specimen is presented in Fig. 7, where an artificial defect was added by 0.1 mm-diameter carbide drilling, with a depth of 0.1 mm, at the minimum cross section. Then, in order to minimize the effect of drilling, 250 °C × 30 min. vacuum heat treatment followed by mirror surface polishing condition of the minimum cross section area by OP-S were conducted. Fatigue tests are operated in air, at room temperature with a rotating speed of 3000 rpm.

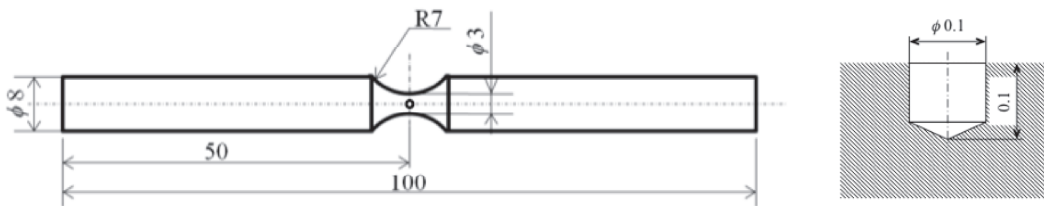


Figure 7: Shape and dimensions of fatigue specimen.

An experiment to assess the performance of the crack length has been undertaken. On a fatigue specimen, where the fatigue crack was already initiated, a comparison has been conducted between the crack length obtained by the system previously introduced and obtained by optical microscopy, where the fatigue test was stopped and bending weight removed (conditions equivalent to the replica method). Observation given by introduced system is presented in Fig. 8(a). Even though the photograph is dark and suffers from lack of clarity, as the bending load tends to open the crack, the crack tip can be easily identified. In this case, this photograph points out a crack length of  $2s = 408 \mu\text{m}$ , considering also the diameter of the artificial defect. On the other hand, after removing the bending weight and extracting the specimen from the testing machine, the photograph Fig. 8(b) has been taken, where the corresponding crack length found is  $2s = 419 \mu\text{m}$ . Thus, even though the length obtained by introduced system is slightly lower, a relative error of approximately 3 % can be noted. The introduced system in this paper is thought to give relevant observation of the fatigue crack.

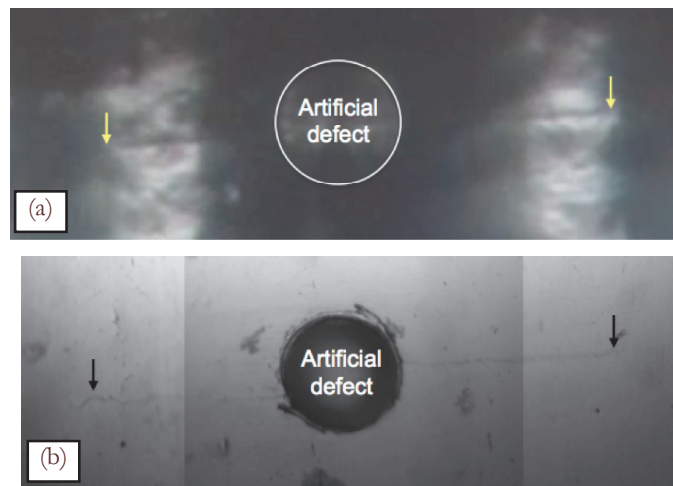


Figure 8: Comparison of fatigue crack images. (a): Fatigue crack image obtained with observing system, (b): Fatigue crack image obtained with optical microscope (No weight and no rotation).

Change of the crack length at different cycle stages for a single specimen subjected to a fatigue test at  $\sigma_a = 800 \text{ MPa}$  ( $N_f = 4.57 \times 10^4$  cycles) stress amplitude is shown in Fig. 9. As the crack propagates, if the observation field of the microscope does no more sufficient to see the entire crack length, it is necessary to switch to the configuration shown in Fig. 5(b). In

such a way, it is possible to record the crack propagation from early stage at the artificial defect to just before the final fracture phenomenon of the specimen.

The crack length measurement results obtained for the experiment using a specimen with an artificial defect ( $\sigma_a = 800$  MPa,  $N_f = 4.57 \times 10^4$  cycles) and using a specimen without artificial defect ( $\sigma_a = 1400$  MPa,  $N_f = 2.39 \times 10^4$  cycles) are depicted in Fig. 10(a) and (b), respectively. Detection of the early stage of the crack propagation is approximately at  $10 \mu\text{m}$  in the case of experiment using a specimen with artificial defect, whereas a length of approximately  $20 \mu\text{m}$  was necessary for specimen without artificial defect.

In the present experiments, the LED stroboscope gives an uneven enlightenment, inducing bright and dark spots along the whole observation field. It is thought that future improvements of the flashing technique would give fatigue crack observations with better clarity.

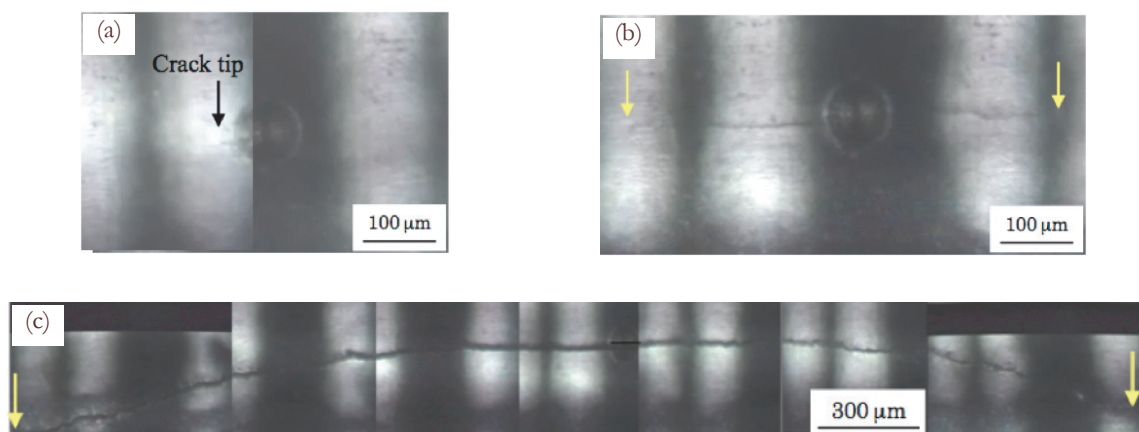


Figure 9: Series images of fatigue crack initiation and propagation. (a):  $N = 7.50 \times 10^3$  cycles, (b):  $N = 3.45 \times 10^4$  cycles,  $2s = 606 \mu\text{m}$ , (c):  $N = 4.50 \times 10^4$  cycles,  $2s = 3360 \mu\text{m}$ .

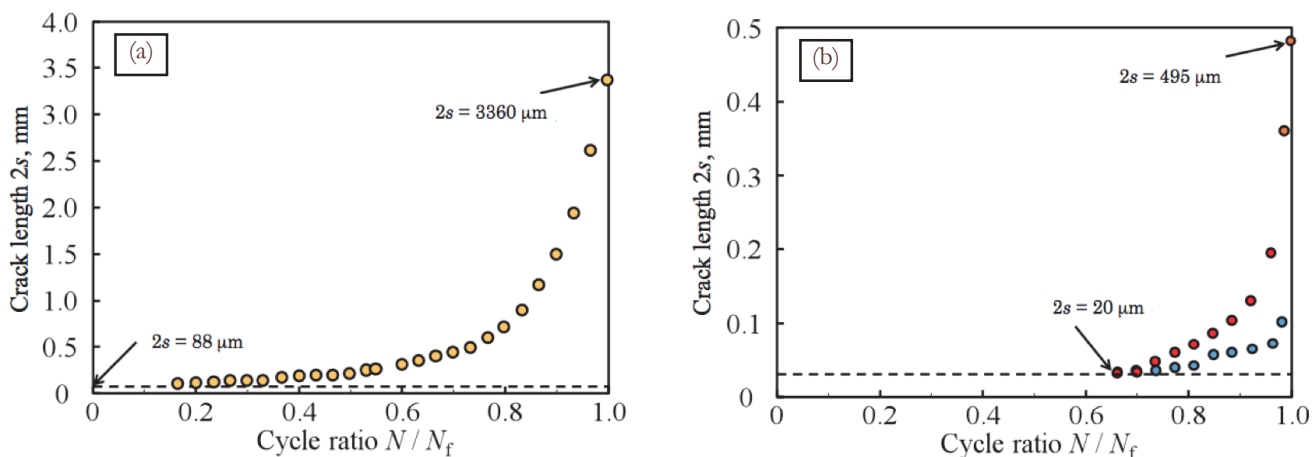


Figure 10: Relationship between cycle ratio and crack length. (a): With artificial defect ( $\sigma_a = 800$  MPa,  $N_f = 4.57 \times 10^4$  cycles), (b): Without artificial defect ( $\sigma_a = 1400$  MPa,  $N_f = 2.39 \times 10^4$  cycles).

## CONCLUSIONS

By using the combination of a LED stroboscope, a control system of the stroboscope flash timing, a long working distance microscope and high spec digital camera, an observation system suitable to record the fatigue crack length on a hourglass shape specimen for rotating bending fatigue tests has been developed. This system allows to study fatigue crack initiation and propagation phenomena at a resolution equivalent to the replica method, without any suspension of the fatigue test.



## REFERENCES

- [1] Lian, B., Fukuchi, Y., Sakaida, A., Ueno, A., Development of high-speed rotating bending fatigue testing machine for evaluating fatigue properties in very high cycle regime, In: Proc. of the 31th JSMS Fatigue Symposium (2012) 56-57, in Japanese.
- [2] Miura, T., Sakakibara, T., Kuno, T., Ueno, A., Kikuchi, S., Sakai, T., Interior-induced fracture mechanism of valve spring steel (JIS SWOSC-V) with high cleanliness in very high cycle regime, In: Proc. of the 6th International Conference on VHCF, Chengdu, China (2014).